

# Distributed Resource Allocation with Binary Decisions via Newton-like Neural Network Dynamics

Tor Anderson<sup>1</sup>   Sonia Martínez<sup>1</sup>

---

## Abstract

This paper aims to solve a distributed resource allocation problem with binary local constraints. The problem is formulated as a binary program with a cost function defined by the summation of agent costs plus a global mismatch/penalty term. We propose a modification of the Hopfield Neural Network (HNN) dynamics in order to solve this problem while incorporating a novel Newton-like weighting factor. This addition lends itself to fast avoidance of saddle points, which the gradient-like HNN is susceptible to. Turning to a multi-agent setting, we reformulate the problem and develop a distributed implementation of the Newton-like dynamics. We show that if a local solution to the distributed reformulation is obtained, it is also a local solution to the centralized problem. A main contribution of this work is to show that the probability of converging to a saddle point of an appropriately defined energy function in both the centralized and distributed settings is zero under light assumptions. Finally, we enlarge our algorithm with an annealing technique which gradually learns a feasible binary solution. Simulation results demonstrate that the proposed methods are competitive with centralized greedy and SDP relaxation approaches in terms of solution quality, while the main advantage of our approach is a significant improvement in runtime over the SDP relaxation method and the distributed quality of implementation.

*Key words:* second-order methods; dynamical systems; distributed optimization; neural networks; binary optimization.

---

## 1 Introduction

There has been an explosion of literature surrounding the design of distributed algorithms for convex optimization problems and how these pertain to the operation of future power grids. A common assumption of these algorithms is the property of *convexity*, which lends itself to provably optimal solutions which are *scalable* and *fast*. However, some settings give rise to nonconvex decision sets. For example, in an optimal power dispatch setting, devices available for providing load-side frequency regulation such as HVAC systems, household appliances, and manufacturing systems are often limited to discrete on/off operational modes. It is even preferable to charge populations of electric vehicles in a discrete on/off manner due to nonlinear battery chemistries. The available tools in optimization for these nonconvex settings are less mature, and when considering a distributed setting in which devices act as agents that collectively compute a solution over a sparse communication graph, the avail-

able tools are significantly less developed. With this in mind, we are motivated to develop a *scalable, fast* approach for these binary settings which is amenable to a *distributed* implementation.

Quadratic programs with nonconvex binary constraints are known to be NP-hard in general, see [7, 22]. In this paper, we consider a problem which is quite applicable to the economic dispatch problem in power networks, see [16, 17, 19] for three recent examples in microgrid environments. However, none of these examples address devices with binary constraint sets. The binary problem is, however, desirable to approach in a distributed context [36, 37]. Greedy algorithms [9] have been proposed for binary programs, such as the well-known Traveling Salesman Problem (TSP), but it is well documented that these methods can greatly suffer in performance [15] except in cases where the cost function is submodular [26, 32]. A more modern approach to solving optimization problems with a binary feasibility set is to cast them as a semidefinite program (SDP) with a nonlinear rank constraint, see [4, 29, 34] for some classical references or [23, 35] for more recent work on the topic. By relaxing the rank constraint, a convex problem is obtained whose solution can be shown to be equal to the optimal dual value of the original problem, see e.g. [28]. However, it is necessary in these approaches to either impose a single centralized coordinator to compute the solution

---

<sup>1</sup> Tor Anderson and Sonia Martínez are with the Department of Mechanical and Aerospace Engineering, University of California, San Diego, CA, USA. Email: {tka001, soniamd}@eng.ucsd.edu. This research was supported by the Advanced Research Projects Agency - Energy under the NODES program, Cooperative Agreement de-ar0000695.

and broadcast it to the actuators or agents, or schedule computations, which suffers from scalability issues, privacy concerns, and does not enjoy the simpler and more robust implementation of a distributed architecture in a large network.

Neuro-dynamic programming is a different paradigm for addressing nonconvex problems with computational tractability, see [3] for a broad reference. A neural-network based method for binary programs was first developed by Hopfield in [18], which was originally proposed in order to address TSPs. We refer to this method from here on as a Hopfield Neural Network (HNN). This method provided a completely different avenue for approaching binary optimizations, and followup works are found in [2, 20, 24, 33]. These works formalize and expand the framework in which the HNN method is applicable. However, these algorithms essentially implement a gradient-descent on an applicable nonconvex energy function, which is susceptible to being slowed down by convergence to saddle-points. There are avenues for Newton-like algorithms in nonconvex environments to address this issue, which incorporate some treatment of the negative Hessian eigenvalues in order to maintain a monotonic descent of the cost function, see e.g. [10, 11]. A recently developed method employs a Positive-definite Truncated inverse (PT-inverse) operation on the Hessian of a nonconvex energy or cost function in order to define a nonconvex Newton-descent direction [31], although the technique does not presently address binary settings. Perhaps more importantly, all variants of existing HNN methods and the aforementioned works for nonconvex Newton-like algorithms are framed for centralized environments in which each agent knows global information about the state of all other agents, which is not scalable.

The contributions of this paper are threefold. We start by considering a binary programming problem formulated as a summation of local costs plus a squared global term. By leveraging a specific choice for the cost functions, we adapt the setting to an HNN framework. Then, we propose a novel modification of the dynamics with a PT-inverse of the Hessian of an appropriate energy function to define centralized NEWTON-LIKE NEURAL NETWORK (NNN-C). We prove a rigorous convergence result to a local minimizer, thus excluding saddle-points, with probability one, given some mild assumptions on the algorithm parameters and initial condition. Thirdly, we reformulate the problem so that it is solvable via a distributed algorithm by means of an auxiliary variable. We show that local solutions of the distributed reformulation are equivalent to local solutions of the centralized one, and we define a corresponding energy function and distributed algorithm for which we show convergence to a local minimizer with probability one. Simulations validate that our method is superior to SDP relaxation approaches in terms of runtime and scalability and outperforms

greedy methods in terms of scalability.

## 2 Preliminaries

This section establishes notation<sup>2</sup> and background concepts to be used throughout the paper.

We refer the reader to [6] as a Graph Theory supplement. One can define a Laplacian matrix  $L$  associated with a graph  $\mathcal{G}$  as follows:

$$L_{ij} = \begin{cases} -1, & j \in \mathcal{N}_i, \\ -\sum_{k \neq i} L_{ik}, & i = j, \\ 0, & \text{otherwise,} \end{cases}$$

where  $\mathcal{N}_i$  is the set of neighbors of node  $i$ . An immediate property is that 0 is an eigenvalue of  $L$  associated with the eigenvector  $\mathbf{1}_n$ . It is simple iff  $\mathcal{G}$  is connected.

Next, we introduce the Positive-definite Truncated inverse (PT-inverse) and its relevance to nonconvex Newton methods.

**Definition 1 ([31]) (PT-inverse).** Let  $A \in \mathbb{R}^{n \times n}$  be a symmetric matrix with an orthonormal basis of eigenvectors  $Q \in \mathbb{R}^{n \times n}$  and diagonal matrix of eigenvalues  $\Lambda \in \mathbb{R}^{n \times n}$ . Consider a constant  $m > 0$  and define  $|\Lambda|_m \in \mathbb{R}^{n \times n}$  by:

$$(|\Lambda|_m)_{ii} = \begin{cases} |\Lambda_{ii}|, & |\Lambda_{ii}| \geq m, \\ m, & \text{otherwise.} \end{cases}$$

The PT-inverse of  $A$  with parameter  $m$  is defined by  $(|A|_m)^{-1} = Q^\top (|\Lambda|_m)^{-1} Q \succ 0$ .

The PT-inverse operation flips the sign on the negative eigenvalues of  $A$  and truncates near-zero eigenvalues to a (small) positive value  $m$  before conducting the

<sup>2</sup> The set of real numbers, real positive numbers, real  $n$ -dimensional vectors, and real  $n$ -by- $m$  matrices are written as  $\mathbb{R}$ ,  $\mathbb{R}_+$ ,  $\mathbb{R}^n$ , and  $\mathbb{R}^{n \times m}$ , respectively. We denote by  $x_i$  the  $i^{\text{th}}$  element of  $x \in \mathbb{R}^n$  and  $A_{ij}$  the element in the  $i^{\text{th}}$  row and  $j^{\text{th}}$  column of  $A \in \mathbb{R}^{n \times m}$ . For a square matrix  $A$ , we denote by  $A^\dagger$  the Moore-Penrose pseudoinverse of  $A$ . We use the shorthand  $\mathbf{1}_n = (1, \dots, 1)^\top \in \mathbb{R}^n$  and  $\mathbf{0}_n = (0, \dots, 0)^\top \in \mathbb{R}^n$ . Cartesian products of sets are denoted by a superscript, for example,  $\{0, 1\}^n = \{0, 1\} \times \dots \times \{0, 1\}$ . The gradient of a function  $f: \mathbb{R}^n \rightarrow \mathbb{R}$  with respect to  $x \in \mathbb{R}^n$  at  $x$  is denoted by  $\nabla_x f(x) \in \mathbb{R}^n$ , and the Hessian matrix of  $f$  at  $x$  is written as  $\nabla_{xx} f(x) \in \mathbb{R}^{n \times n}$ . We denote elementwise operations on vectors  $x, y \in \mathbb{R}^n$  as  $(x_i y_i)_i = (x_1 y_1, \dots, x_n y_n)^\top$ ,  $(x_i)^2_i = (x_1^2, \dots, x_n^2)^\top$ ,  $(c/x_i)_i = (c/x_1, \dots, c/x_n)^\top$ ,  $\log(x_i)_i = (\log(x_1), \dots, \log(x_n))^\top$ , and  $(e^{x_i})_i = (e^{x_1}, \dots, e^{x_n})^\top$ . The notation  $\text{diag}(x)$  indicates the diagonal matrix with entries given by elements of  $x$ , and  $\mathcal{B}(x, \eta)$  denotes the closed ball of radius  $\eta$  centered at  $x$ .

inverse. Effectively, this generates a positive definite matrix bounded away from zero to be inverted, circumventing near-singular cases. In terms of computational complexity, it is on the order of standard eigendecomposition (or more generally, singular value decomposition), which is roughly  $O(n^3)$  [27]. However, we note in Section 5 that the matrix to be PT-inverted is diagonal, which is  $O(n)$ .

The PT-inverse is useful for nonconvex Newton approaches [31] in the following sense: first, recall that the Newton descent direction of  $f$  at  $x$  is computed as  $-(\nabla_{xx}f(x))^{-1}\nabla_x f(x)$ . For  $f$  strictly convex, it holds that  $\nabla_{xx}f(x) \succ 0$  and the Newton direction is well defined and decreases the cost. For (non-strictly) convex or nonconvex cases,  $\nabla_{xx}f(x)$  will be singular, indefinite, or negative definite. A PT-inverse operation remedies these cases and preserves the descent quality of the method. Additionally, saddle points are a primary concern for first-order methods in nonconvex settings [10], and the Newton flavor endowed by the PT-inverse effectively performs a change of coordinates on saddles with “slow” unstable manifolds compared to the stable manifolds. We discuss this further in Section 4.

### 3 Problem Statement and Dual Problem

Here, we formally state the nonconvex optimization problem we wish to solve and formulate its dual for the sake of deriving a lower bound to the optimal cost.

We aim to find an adequate solution to a resource allocation problem where the optimization variables take the form of binary decisions over a population of  $n$  agents. We note that the problem we consider is applicable to generator dispatch and active device response in an economic dispatch power systems setting [1], but the remainder of the paper will frame it primarily as resource allocation. Let each agent  $i \in \{1, \dots, n\}$  be endowed with a decision variable  $x_i$  and a cost  $c_i \in \mathbb{R}$ , a value which indicates the incremental cost of operating in the  $x_i = 1$  state versus the  $x_i = 0$  state. We do not impose a sign restriction on  $c_i$ , but this may be a common choice in the power systems setting where  $x_i = 1$  represents an “on” device state and  $x_i = 0$  represents “off.” Additionally, each agent is endowed with a parameter  $p_i$  which represents some incremental consumption or generation quantity when operating in the  $x_i = 1$  state versus  $x_i = 0$  and also a passive cost  $d_i$ .

We are afforded some design choice in the cost function models for  $x_i \notin \{0, 1\}$ , and for each  $i \in \{1, \dots, n\}$ , so we design abstracted cost functions  $f_i : [0, 1] \rightarrow \mathbb{R}$  that satisfy  $f_i(0) = d_i$  and  $f_i(1) = c_i + d_i, \forall i$ . This design choice is intrinsic to a cost model for any separable binary decision optimization context. In particular, the value of  $f_i(x_i)$  for any  $x_i \notin \{0, 1\}$  is only relevant to the algorithm design, but need not have a physical interpretation or pertain to the optimization model since these

points are infeasible. With this in mind, we enlarge the cost model by adopting the following:

**Assumption 1 (Quadratic Cost Functions).** *The local cost functions  $f_i$  take the form*

$$f_i(x_i) = \frac{a_i}{2}(x_i - b_i)^2 - \frac{a_i b_i^2}{2} + d_i,$$

with  $a_i, b_i, d_i \in \mathbb{R}$ .

Note that, for any value  $c_i = f_i(1) - f_i(0)$ , there exists a family of coefficients  $a_i, b_i$  such that  $(a_i/2)(1 - b_i)^2 - (a_i/2)b_i^2 = c_i$ . Further, the constant terms ensure  $f_i(0) = d_i$  and  $f_i(1) = c_i + d_i$ . The design of  $a_i, b_i$  will be discussed in Section 4.

The problem we aim to solve can now be formulated as:

$$\mathcal{P}1 : \min_{x \in \{0,1\}^n} f(x) = \sum_i^n f_i(x_i) + \frac{\gamma}{2} (p^\top x - P_r)^2.$$

Here,  $P_r \in \mathbb{R}$  is a given reference value to be matched by the total output  $p^\top x$  of the devices, with  $p \in \mathbb{R}^n$  having entries  $p_i$ . This matching is enforced by means of a penalty term with coefficient  $\gamma > 0$  in  $\mathcal{P}1$ . In the power systems setting,  $P_r$  can represent a real-power quantity to be approximately matched by the collective device-response. The coefficient  $\gamma$  and the signal  $P_r$  are determined by an Independent System Operator (ISO) and communicated to a Distributed Energy Resource Provider (DERP) that solves  $\mathcal{P}1$  to obtain a real-time dispatch solution, see [1] for additional information.

The primal  $\mathcal{P}1$  has an associated dual  $\mathcal{D}1$  which takes the form of a semidefinite program (SDP) whose optimal value lower bounds the cost of  $\mathcal{P}1$ . This SDP is

$$\mathcal{D}1 : \max_{\mu \in \mathbb{R}^n, \Delta \in \mathbb{R}} \Delta, \tag{1a}$$

$$\text{subject to} \quad \begin{bmatrix} \frac{1}{2}Q(\mu) & \xi(\mu) \\ \xi(\mu)^\top & \zeta - \Delta \end{bmatrix} \succeq 0. \tag{1b}$$

In  $\mathcal{D}1$ ,  $Q : \mathbb{R}^n \rightarrow \mathbb{R}^{n \times n}$  and  $\xi : \mathbb{R}^n \rightarrow \mathbb{R}^n$  are real-affine functions of  $\mu$  and  $\zeta$  is a constant. These definitions are  $Q(\mu) = \left( \text{diag}(a/2 + \mu) + \frac{\gamma}{2}pp^\top \right)$ ,  $\xi(\mu) = ((a_i b_i)_i + \mu + \gamma P_r p)$ , and  $\zeta = \sum_{i=1}^n \frac{a_i b_i^2}{2} + \frac{\gamma}{2} P_r^2$ . See [5] for more detail on the derivation of  $\mathcal{D}1$ .

### 4 Centralized Newton-like Neural Network

In this section, we develop the Centralized NEWTON-LIKE NEURAL NETWORK, or NNN-C, which is well suited for solving  $\mathcal{P}1$  in a centralized setting.

To draw analogy with the classic Hopfield Neural Network approach we will briefly introduce an auxiliary variable  $u_i$  whose relation to  $x_i$  is given by the logistic function  $g$  for each  $i$ :

$$\begin{aligned} x_i &= g(u_i) = \frac{1}{1 + e^{-u_i/T}}, & u_i &\in \mathbb{R}, & (2) \\ u_i &= g^{-1}(x_i) = -T \log\left(\frac{1}{x_i} - 1\right), & x_i &\in (0, 1), \end{aligned}$$

with temperature parameter  $T > 0$ .

Let  $x \in (0, 1)^n, u \in \mathbb{R}^n$  be vectors with entries given by  $x_i, u_i$ . To establish our algorithm, it is appropriate to first define an energy function related to  $\mathcal{P} 1$ . Consider

$$E(x) = f(x) + \frac{1}{\tau} \sum_i \int_0^{x_i} g^{-1}(\nu) d\nu, \quad (3)$$

where  $\tau > 0$  is a time-constant and for  $z \in [0, 1]$ ,

$$\int_0^z g^{-1}(\nu) d\nu = \begin{cases} T (\log(1-z) - z \log(\frac{1}{z} - 1)), & z \in (0, 1), \\ 0, & z \in \{0, 1\}. \end{cases}$$

The classic HNN implements dynamics of the form  $\dot{u} = -\nabla_x E(x)$ , where the equivalent dynamics in  $x$  can be computed as  $\dot{x} = -\nabla_x E(x) dx/du$ . These dynamics can be thought of to model the interactions between neurons in a neural network or the interconnection of amplifiers in an electronic circuit, where in both cases the physical system tends toward low energy states, see [18, 33]. In an optimization setting, low energy states draw analogy to low cost solutions. We now describe our modification to the classical HNN dynamics.

Recall that the domain of  $x$  is  $(0, 1)^n$  and our elementwise notation for log and division. We have the expressions  $\nabla_x E(x) = -Wx - v - (T/\tau) \log(1/x_i - 1)_i$  and  $dx/du = (x - (x_i^2)_i)/T$ , where  $W = -\text{diag}(a) - \gamma pp^T \in \mathbb{R}^{n \times n}$  and  $v = (a_i b_i)_i + \gamma P_r p \in \mathbb{R}^n$  are defined via  $f$ . From this point forward, we work mostly in terms of  $x$  for the sake of consistency. Consider modifying the classic HNN dynamics with a PT-inverse  $(|H(x)|_m)^{-1} \succ 0$  as in [31], where  $H(x) = \nabla_{xx} E(x)$ . The NNN-C dynamics are then given by:

$$\begin{aligned} \dot{x} &= -(|H(x)|_m)^{-1} \text{diag}\left(\frac{dx}{du}\right) \nabla_x E(x) \\ &= (|H(x)|_m)^{-1} \text{diag}\left(\frac{(x_i - x_i^2)_i}{T}\right) \\ &\quad \left(Wx + v + \frac{T}{\tau} \log(1/x_i - 1)_i\right). \end{aligned} \quad (4)$$

These dynamics lend to the avoidance of saddle points of  $E$ . To see this, consider the eigendecomposition  $H(\tilde{x}) =$

$Q^T \Lambda Q$  at some  $\tilde{x}$  near a saddle point, i.e.  $\nabla_x E(\tilde{x}) \approx 0$ . If many entries of  $\Lambda$  are small in magnitude and remain small in the proximity of  $\tilde{x}$ , then the gradient is changing slowly along the ‘‘slow’’ manifolds associated with the eigenspace of the small eigenvalues. This is precisely what the PT-inverse is designed to combat: the weighting of the dynamics is increased along these manifolds by a factor that is inversely proportional to the magnitude of the eigenvalues. Additionally, negative eigenvalues of the Hessian are flipped in sign, which causes attractive manifolds around saddle points to become repellent.

It is desirable for  $E$  to be concave on most of its domain so the trajectories are pushed towards the feasible points of  $\mathcal{P} 1$ ; namely, the corners of the unit hypercube. To examine this, the Hessian of  $E$  can be computed as  $H(x) = \frac{d^2 f}{dx^2} + \frac{1}{\tau} \text{diag}\left(\frac{dg^{-1}(x)}{dx}\right) = -W + \frac{T}{\tau} \text{diag}\left(\frac{1}{(x_i - x_i^2)_i}\right)$ . Notice that the second term is positive definite on  $x \in (0, 1)^n$  and promotes the convexity of  $E$ , particularly for elements  $x_i$  close to 0 or 1. For a fixed  $T, \tau$ , choosing  $a_i < -\gamma \|p\|^2 - 4T/\tau, \forall i$  guarantees  $E(x) < 0$  at  $x = (0.5) \mathbf{1}_n$ . Generally speaking, choosing  $a_i$  to be negative and large in magnitude lends itself to concavity of  $E$  over a larger subset of its domain and to trajectories converging closer to the set  $\{0, 1\}^n$ . However, this comes at the expense of not exploring a rich subset of the domain. At the end of this section, we develop a Deterministic Annealing (DA) approach inspired by [30] for the online adjustment of  $T, \tau$  to obtain an effective compromise between exploration of the state space and convergence to a feasible point of  $\mathcal{P} 1$ .

We now characterize the equilibria of (4) for  $x \in [0, 1]^n$ . It would appear that  $x$  with some components  $x_i \in \{0, 1\}$  are candidate equilibria due to the  $x_i - x_i^2$  factor vanishing. However, the dynamics are not well defined here due to the log term. Additionally, note that  $\lim_{x_i \rightarrow \delta} e_i^T H(x) e_i = \infty, \delta \in \{0, 1\}, \forall i$ , where  $e_i$  is the  $i^{\text{th}}$  canonical basis vector. Due to the  $\frac{T}{\tau(x_i - x_i^2)}$  term dominating  $W$  in the expression for  $H$  when  $x_i$  values are close to  $\{0, 1\}$ , it follows that an eigenvalue of  $(|H(x)|_m)^{-1}$  approaches zero as  $x_i \rightarrow 0$  or 1 with corresponding eigenvector approaching  $v_i = e_i$ :

$$\lim_{x_i \rightarrow \delta} v_i^T (|H(x)|_m)^{-1} v_i = \frac{T}{\tau} (x_i - x_i^2) = 0, \quad \delta \in \{0, 1\}, \forall i.$$

Using this fact, and ignoring  $T, \tau > 0$ , we can compute the undetermined limits in the components of  $\dot{x}$  as  $x_i \rightarrow \delta \in \{0, 1\}$  by repeated applications of L’Hospital’s rule:

$$\lim_{x_i \rightarrow \delta} \log\left(\frac{1}{x_i} - 1\right) (x_i - x_i^2)^2 = \begin{cases} 0, & \delta = 0^+, \\ 0, & \delta = 1^-. \end{cases} \quad (5)$$

Thus, components  $x_i \in \{0, 1\}$  constitute candidate equilibria. We will, however, return to the first line of (5) in the proof of Lemma 3 to show that they are unstable. As

for components of  $x$  in the interior of the hypercube, the expression  $\dot{x} = 0$  can not be solved for in closed form. However, we provide the following Lemma which shows that the set of equilibria is finite.

**Lemma 2 (Finite Equilibria).** *Let  $\mathcal{X}$  be the set of equilibria of (4) satisfying  $\dot{x} = 0$  on  $x \in [0, 1]^n$ . The set  $\mathcal{X}$  is finite.*

The proof can be found in the Appendix, and all proofs for the remainder of the paper will be contained there.

To demonstrate the qualitative behavior of equilibria in a simple case, consider a one-dimensional example with  $a > -\gamma p^2 - 4T/\tau$  and recall that, for  $x \in (0, 1)$ , the sign of  $-\nabla_x E(x)$  is the same as  $\dot{x}$ . In Figure 1, we observe that  $-\nabla_x E(x)$  monotonically decreases in  $x$ , and a globally stable equilibrium exists in the interior  $x \in (0, 1)$  near  $x = 0.5$ . On the other hand,  $a < -\gamma p^2 - 4T/\tau$  gives way to 3 isolated equilibria in the interior (one locally unstable near  $x = 0.5$  and two locally stable near  $x \in \{0, 1\}$ ). This behavior extends in some sense to the higher-dimensional case. Therefore, for a scheme in which  $T$  and  $\tau$  are held fixed, we prescribe  $a < -\gamma\|p\|^2 - 4T/\tau$ . We provide a Deterministic Annealing (DA) approach inspired by [30] for the on-line adjustment of  $T, \tau$  in the following subsection which compromises with this strict design of  $a$ .

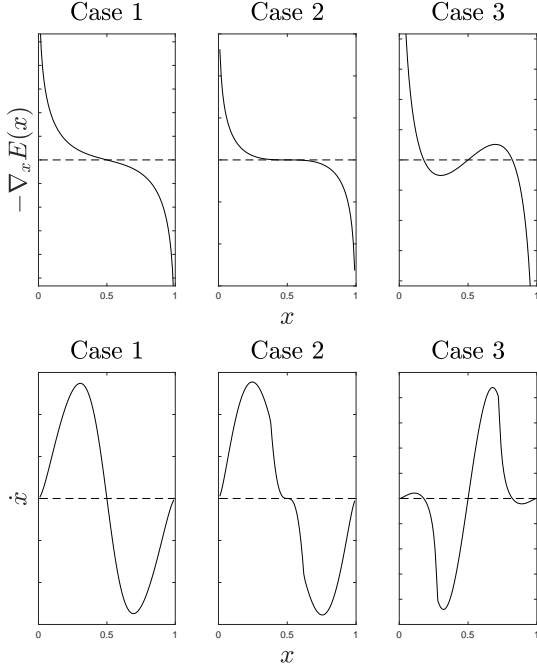


Fig. 1. Illustration of  $-\nabla_x E(x)$  (top) and  $\dot{x}$  (bottom) for three instances of  $a$ . Case 1:  $a > -\gamma\|p\|^2 - 4T/\tau$ , Case 2:  $a = -\gamma\|p\|^2 - 4T/\tau$ , Case 3:  $a < -\gamma\|p\|^2 - 4T/\tau$ .

Finally, we establish a Lemma about the domain of the trajectories of (4).

**Lemma 3 (Forward Invariance of the Open Hypercube).** *The open hypercube  $(0, 1)^n$  is a forward-invariant set under the NNN-C dynamics (4).*

Knowing that  $\mathcal{P} 1$  is generally NP-hard, it is unlikely that a non-brute-force algorithm exists that can converge to a global minimizer. For this reason, we aim to establish asymptotic stability to a local minimizer of  $E$ . We first establish some assumptions.

**Assumption 2 (Random Initial Condition).** *The initial condition  $x(0)$  is chosen randomly according to a distribution  $\mathbb{P}$  that is nonzero on sets that have nonzero volume in  $[0, 1]^n$ .*

An appropriately unbiased initial condition for our algorithm is  $x(0) \approx (0.5) \mathbf{1}_n$ , which is adequately far from the local minima located near corners of the unit cube. So, we suggest choosing a uniformly random  $x(0) \in \mathcal{B}((0.5) \mathbf{1}_n, \epsilon)$ , where  $0 < \epsilon \ll 1$ .

**Assumption 3 (Choice of  $T, \tau$ ).** *The constants  $T, \tau > 0$  are each chosen randomly according to a distribution  $\mathbb{P}$  that is nonzero on sets that have nonzero volume on  $\mathbb{R}_+$ .*

Similarly to  $x(0)$ , we suggest choosing these constants uniformly randomly in a ball around some nominal  $T_0, \tau_0$ , i.e.  $T \in \mathcal{B}(T_0, \epsilon), \tau \in \mathcal{B}(\tau_0, \epsilon), 0 < \epsilon \ll 1$ . The  $T_0, \tau_0$  themselves are design parameters stemming from the neural network model, and we provide some intuition for selecting these in the simulation Section.

Now we state the main convergence result of NNN-C in Theorem 4, which states that for a random choice of  $T, \tau$ , an initial condition chosen randomly from  $(0, 1)^n$  converges asymptotically to a local minimizer of  $E$  with probability one.

**Theorem 4 (Convergence of NNN-c).** *Given an initial condition  $x(0) \in (0, 1)^n$ , the trajectory  $x(t)$  under NNN-C converges asymptotically to a critical point  $x^*$  of  $E$ . In addition, under Assumption 2, on the random choice of initial conditions, and Assumption 3, on the random choice of  $T, \tau$ , the probability that  $x(0)$  is in the set  $\cup_{\hat{x}} \mathcal{W}^s(\hat{x})$ , where  $\hat{x}$  is a saddle-point or local maximum of  $E$ , is zero.*

We now define a Deterministic Annealing (DA) variant inspired by [30] to augment the NNN-C dynamics and provide a method for gradually learning a justifiably good feasible point of  $\mathcal{P} 1$ . In [30], the author justifies the deterministic online tuning of a temperature parameter in the context of data clustering and shows that this avoids poor local optima by more thoroughly exploring the state space. Similarly, we aim to learn a sufficiently good solution trajectory by allowing the dynamics to explore the interior of the unit hypercube in

the early stages of the algorithm, and then to force the trajectory outward to a feasible binary solution by gradually adjusting  $T$  or  $\tau$  online.

Consider either reducing the temperature  $T$  or increasing the time constant  $\tau$  during the execution of NNN-C. This reduces the terms in  $E$  which promote convexity, particularly near the boundaries of the unit hypercube. As  $T, \tau$  are adjusted, for  $a \prec -\gamma\|p\|^2$ , the domain of  $E$  becomes gradually more concave away from the corners of the unit hypercube. Thus, starting with  $T/\tau$  sufficiently large, the early stages of the algorithm promote exploration of the interior of the state space. As  $T/\tau$  is reduced, the equilibria of  $E$  are pushed closer to (and eventually converge to) the feasible points of  $\mathcal{P} 1$ . The update policy we propose is described formally in Algorithm 1, and we further explore its performance in simulation.

---

**Algorithm 1** Deterministic Annealing

---

- 1: **procedure** DET-ANNEAL( $\beta > 1, T_0, \tau_0, t_d$ )
  - 2:     Initialize  $x(0)$
  - 3:      $T \leftarrow T_0, \tau \leftarrow \tau_0$
  - 4:     **while true do**
  - 5:         Implement NNN-C for  $t_d$  seconds
  - 6:          $\tau \leftarrow \beta\tau$    or    $T \leftarrow (1/\beta)T$
  - 7:     **end while**
  - 8: **end procedure**
- 

Note that Algorithm 1 leads to a hybrid dynamic system with discrete jumps in an enlarged state  $\phi = (x, T, \tau)$ , which can cast some doubt on basic existence and uniqueness of solutions. We refer the reader to Propositions 2.10 and 2.11 of [12] to justify existence and uniqueness of solutions in the case of  $t_d > 0$  fixed.

**Corollary 5 (Convergence to Feasible Points).** *Under Assumptions 2-3 and  $a \prec -\gamma\|p\|^2$ , the NNN-C dynamics augmented with Algorithm 1 converge asymptotically to feasible points of  $\mathcal{P} 1$ .*

The result of the Corollary is quickly verified by inspecting the terms of  $H(x)$ . The function  $E$  is smooth, strictly concave near  $x = (0.5) \mathbf{1}_n$  for small  $T/\tau$  due to the design of  $a_i$ , and becomes strictly convex as the elements of  $x$  approach 0 or 1, corresponding to isolated local minima of  $E$ , due to the  $T/\tau$  term dominating  $H(x)$ . As the quantity  $T/\tau$  is reduced under Algorithm 1, these local minima are shifted asymptotically closer to corners of the unit hypercube, i.e. feasible points of  $\mathcal{P} 1$ .

## 5 Distributed Hopfield Neural Network

With the framework of the previous section we formulate a problem  $\mathcal{P} 2$  which is closely related to  $\mathcal{P} 1$ , but for which the global penalty term can be encoded by means of an auxiliary decision variable. This formulation leads

to the Distributed NEWTON-LIKE NEURAL NETWORK, or NNN-D, which we rigorously analyze for its convergence properties.

It is clear from the PT-inverse operation and  $W$  being nonsparse that NNN-C is indeed centralized. In this section, we design a distributed algorithm in which each agent  $i$  must only know  $p_j, j \in \mathcal{N}_i$  and the value of an auxiliary variable  $y_j, j \in \mathcal{N}_i \cup \mathcal{N}_i^2$ , i.e. it must have communication with its two-hop neighbor set. If two-hop communications are not directly available, the algorithm can be implemented with two communication rounds per algorithm step. We provide comments on a one-hop algorithm in Remark 12.

**Assumption 4 (Graph Properties and Connectivity).** *The graph  $\mathcal{G} = (\mathcal{N}, \mathcal{E})$  is undirected and connected; that is, a path exists between any two pair of nodes and, equivalently, its associated Laplacian matrix  $L = L^\top$  has rank  $n - 1$ .*

Now consider the  $n$  linear equations  $(p_i x_i)_i + Ly = (P_r/n) \mathbf{1}_n$ . Notice that, by multiplying from the left by  $\mathbf{1}_n^\top$  and applying  $\mathbf{1}_n^\top L = \mathbf{0}_n^\top$ , we recover  $p^\top x = P_r$ . Thus, by augmenting the state with an additional variable  $y \in \mathbb{R}^n$ , we can impose a distributed penalty term. We now formally state the distributed reformulation of  $\mathcal{P} 1$ :

$$\mathcal{P} 2 : \quad \min_{x \in \{0,1\}^n, y \in \mathbb{R}^n} \tilde{f}(x, y) = \sum_i^n f_i(x_i) + \frac{\gamma}{2} \sigma^\top \sigma,$$

where the costs  $f_i$  again satisfy  $f_i(1) - f_i(0) = c_i$  and we have defined  $\sigma = (p_i x_i)_i + Ly - (P_r/n) \mathbf{1}_n$  for notational simplicity. Before proceeding, we provide some context on the relationship between  $\mathcal{P} 1$  and  $\mathcal{P} 2$ .

**Lemma 6 (Equivalence of  $\mathcal{P} 1$  and  $\mathcal{P} 2$ ).** *Let Assumption 4, on graph connectivity, hold, and let  $(x^*, y^*)$  be a solution to  $\mathcal{P} 2$ . Then,  $x^*$  is a solution to  $\mathcal{P} 1$  and  $f(x^*) = \tilde{f}(x^*, y^*)$ .*

To define NNN-D, we augment the centralized NNN-C with gradient-descent dynamics in  $y$  on a newly obtained energy function  $\tilde{E}$  of  $\mathcal{P} 2$ . Define  $\tilde{E}$  as

$$\tilde{E}(x, y) = \tilde{f}(x, y) + \frac{1}{\tau} \sum_i \int_0^{x_i} g^{-1}(\nu) d\nu. \quad (6)$$

In Section 4, we obtained a matrix  $W$  which was nonsparse. Define  $\tilde{W}, \tilde{v}$  for  $\tilde{E}$  via  $\tilde{f}$  as  $\tilde{W} = -\text{diag}(a + \gamma(p_i^2)_i), \tilde{v} = (a_i b_i)_i + \gamma \text{diag}(p) ((P_r/n) \mathbf{1}_n - Ly)$ . Compute the Hessian of  $\tilde{E}$  with respect to only  $x$  as  $\tilde{H}(x) = \nabla_{xx} \tilde{E}(x, y) = -\tilde{W} + (T/\tau) \text{diag}(1/x - (x_i^2)_i)$ . Since  $\tilde{H}(x)$  is diagonal, the  $ii^{\text{th}}$  element of the PT-inverse of  $\tilde{H}(x)$

can be computed locally by each agent  $i$  as:

$$(|\tilde{H}(x)|_m)_{ii}^{-1} = \begin{cases} |\tilde{H}(x)_{ii}|^{-1}, & |\tilde{H}(x)_{ii}| \geq m, \\ 1/m, & \text{o.w.} \end{cases}$$

where  $\tilde{H}(x)_{ii} = a_i + \gamma p_i^2 + T/\tau(x_i - x_i^2)^{-1}$ . The NNN-D dynamics, which are PT-Newton descent in  $x$  and gradient descent in  $y$  on  $\tilde{E}$ , are then stated as:

$$\begin{aligned} \dot{x} &= (|\tilde{H}(x)|_m)^{-1} \text{diag}\left(\frac{(x_i - x_i^2)_i}{T}\right) \\ &\quad \left(\tilde{W}x + \frac{T}{\tau} \log(1/x_i - 1)_i + \tilde{v}\right), \quad (7) \\ \dot{y} &= -\alpha\gamma L((p_i x_i)_i + Ly), \end{aligned}$$

Due to the new matrices  $\tilde{W}, \tilde{v}$  and the sparsity of  $L$ ,  $\dot{x}$  can be computed with one-hop information and  $\dot{y}$  with two-hop information (note the  $L^2$  term); thus, (7) defines a distributed algorithm. Additionally, recalling the discussion on parameter design, the problem data  $a$  and  $b$  can now be locally designed.

Before proceeding, we establish a property of the domain of  $y$  and some distributed extensions of Lemmas 2 and 3.

**Lemma 7 (Domain of Auxiliary Variable).** *Given an initial condition  $y(0)$  with  $\mathbf{1}_n^\top y(0) = \kappa$ , the trajectory  $y(t)$  is contained in the set*

$$\mathcal{Y} = \{\omega + (\kappa/n) \mathbf{1}_n \mid \mathbf{1}_n^\top \omega = 0\}. \quad (8)$$

**Lemma 8 (Closed Form Auxiliary Solution).** *For an arbitrary fixed  $x \in [0, 1]^n$ , the unique minimizer  $y^*$  contained in  $\mathcal{Y}$  of both  $\tilde{f}$  and  $\tilde{E}$  is given by*

$$y^* = -L^\dagger(p_i \tilde{x}_i)_i + \frac{\kappa}{n} \mathbf{1}_n. \quad (9)$$

*This is also the unique equilibrium of (7) in  $\mathcal{Y}$ .*

**Lemma 9 (Finite Equilibria (Distributed)).** *Let  $\tilde{\mathcal{X}} \times \tilde{\mathcal{Y}}$  be the set of equilibria of (7) satisfying  $(\dot{x}, \dot{y}) = 0$  on  $(x, y) \in [0, 1]^n \times \mathcal{Y}$ . The set  $\tilde{\mathcal{X}} \times \tilde{\mathcal{Y}}$  is finite.*

We now extend the results of Theorem 4 to the distributed case of solving  $\mathcal{P} 2$  via NNN-D. We have the following theorem on the trajectories of  $(x(t), y(t))$  under (7), which can be interpreted as establishing convergence to a local minimizer with probability one.

**Theorem 10 (Convergence of NNN-d).** *Given an initial condition  $(x(0), y(0)) \in (0, 1)^n \times \mathbb{R}^n$ , the trajectory  $(x(t), y(t))$  under NNN-D converges asymptotically to a critical point  $(x^*, y^*)$  of  $\tilde{E}$ . In addition, under Assumption 2, on the random choice of initial condition*

$x(0)$ , and Assumption 3, on the random choice of  $T, \tau$ , the probability that  $(x(0), y(0))$  is in the set  $\cup_{\hat{x}, \hat{y}} \mathcal{W}^s(\hat{x}, \hat{y})$ ,

where  $(\hat{x}, \hat{y})$  is a saddle-point or local maximum of  $\tilde{E}$ , is zero. Lastly, all local minima  $(x^*, y^*)$  of  $\tilde{E}$  are globally optimal in  $y$ :  $\tilde{E}(x^*, y) \geq \tilde{E}(x^*, y^*), \forall y \in \mathbb{R}^n$ .

**Lemma 11 (Forward Invariance of the Open Hypercube (Distributed)).** *The set  $(0, 1)^n \times \mathcal{Y}$  is a forward-invariant set under the NNN-D dynamics (7).*

**Remark 12 (One-Hop Distributed Algorithm).**

The proposed distributed algorithm requires two-hop neighbor information, which may be intractable in some settings. The source of the two-hop term stems from the quadratic  $\gamma$  penalty term. However, it is possible to define a one-hop distributed algorithm via a Lagrangian-relaxation route.

Consider posing  $\mathcal{P} 2$  with the  $\gamma$  term instead as a linear constraint:  $\sqrt{\gamma/2}((p_i x_i)_i + Ly) = \sqrt{\gamma/2}(P_i/n) \mathbf{1}_n$ . Applying Lagrangian relaxation to this problem introduces a Lagrange multiplier on the linear terms, and from there it would be appropriate to define a saddle-point-like algorithm along the lines of [8] in which gradient-ascent in the dual variable is performed. This changes the nature of the penalty from squared to linear, so the underlying optimization model is different in that sense, but it follows that this approach could be implemented with one-hop information.

We note that, in some distributed contexts, penalty terms or constraints can be imposed via  $\sqrt{L}$  which then appears as  $L$  in the associated squared terms of the dynamics (in place of  $L^2$ ). However, the linear  $L$  also appears in our algorithm, and substituting  $\sqrt{L}$  would not inherit the sparsity of the communication graph. Therefore we leave the design of a fully one-hop mixed first-order/second-order algorithm as an open problem.

## 6 Simulations

Our simulation study is split in to two parts; the first focuses on numerical comparisons related to runtime and solution quality, and the second is a 2D visualization of the trajectories of the Distributed Annealing (DA) variants for both the centralized and distributed NNN methods.

### 6.1 Runtime and Solution Quality Comparison

In this section, we compare to a greedy method stated as Algorithm 2 and a semidefinite programming (SDP) relaxation method stated as Algorithm 3. In short, the greedy method initializes the state as  $x = \mathbf{0}_n$  and iteratively sets the element  $x_i$  to one which decreases the cost function the most. This is repeated until no element

remains for which the updated state has lower cost than the current state. For the SDP method, a convex SDP is obtained as the relaxation of  $\mathcal{P} 1$ , see e.g. [34]. We use the shorthand  $\text{SDPr1x}(\bullet)$  to indicate this in the statement of Algorithm 3. This SDP is solved using CVX software in MATLAB [13] and a lowest-cost partition is computed to construct a feasible solution. For the sake of convenience in stating both algorithms, we have defined  $f' : 2^n \rightarrow \mathbb{R}$  to be the set function equivalent of  $f$ , i.e. the cost of  $\mathcal{P} 1$ . That is,  $f'(\mathcal{S}) = f(x)$ , where  $i \in \mathcal{S}$  indicates  $x_i = 1$  and  $i \notin \mathcal{S}$  indicates  $x_i = 0$ . Finally, we additionally compare to a brute force method which we have manually programmed as an exhaustive search over the entire (finite) feasibility set.

---

**Algorithm 2** Greedy Method

---

```

1: procedure GREEDY( $f'$ )
2:    $\mathcal{S} \leftarrow \emptyset$ 
3:   done  $\leftarrow$  false
4:   while done = false do
5:      $i^* \leftarrow \underset{i \notin \mathcal{S}}{\text{argmin}} f'(\mathcal{S} \cup \{i\})$ 
6:     if  $f'(\mathcal{S} \cup \{i^*\}) < f'(\mathcal{S})$  then
7:        $\mathcal{S} \leftarrow \mathcal{S} \cup \{i^*\}$ 
8:     else
9:       done  $\leftarrow$  true
10:    end if
11:  end while
12:   $x_i \leftarrow \begin{cases} 0, & i \notin \mathcal{S}, \\ 1, & i \in \mathcal{S}. \end{cases}$ 
13:  return  $x$ 
14: end procedure

```

---

**Algorithm 3** SDP Relaxation Method

---

```

1: procedure SDP( $f'$ )
2:    $\mathcal{P}_{\text{SDP}} \leftarrow \text{SDPr1x}(\mathcal{P} 1)$ 
3:    $x^* \leftarrow \underset{x}{\text{argmin}} \mathcal{P}_{\text{SDP}}$ 
4:    $\mathcal{S} \leftarrow \emptyset$ 
5:   done  $\leftarrow$  false
6:   while done = false do
7:      $i^* \leftarrow \underset{i \notin \mathcal{S}}{\text{argmax}} x_i$ 
8:     if  $f'(\mathcal{S} \cup \{i^*\}) < f'(\mathcal{S})$  then
9:        $\mathcal{S} \leftarrow \mathcal{S} \cup \{i^*\}$ 
10:    else
11:      done  $\leftarrow$  true
12:    end if
13:  end while
14:   $x_i \leftarrow \begin{cases} 0, & i \notin \mathcal{S}, \\ 1, & i \in \mathcal{S}. \end{cases}$ 
15:  return  $x$ 
16: end procedure

```

---

In Figure 2 we plot the runtime in MATLAB on a 3.5GHz Intel Xeon E3-1245 processor over increasing problem size  $n$  for each of six methods: a brute force search, the aforementioned greedy and SDP methods, the HNN first proposed in [18] (i.e. the gradient-like version of

NNN-c), and the NNN-C and NNN-D methods we developed in Sections 4 and 5. The first obvious observation to make is that the runtime of brute force method increases at a steep exponential rate with increasing  $n$  and exceeds 120 seconds at  $n = 22$ , making it intractable for even medium sized problems. Next, we note that there are some spikes associated with the HNN method around  $n = 25$  to  $n = 40$ . These are reproducible, and we suspect that this is due to the emergence of saddle-points and increasing likelihood of encountering these along the trajectory as  $n$  increases. This is a well-documented problem observed in literature, see e.g. [10], and we also confirm it empirically in this setting by observing that share of iterations for which the Hessian is indefinite (as opposed to positive definite) tends to grow as  $n$  increases. We also note that NNN-C scales relatively poorly, which can be attributed to a matrix eigen-decomposition being performed at each discretized iteration of the continuous-time algorithm. For NNN-D, the matrix being eigendecomposed is diagonal, which makes it a trivial operation and allows NNN-D to scale well. We note that the SDP method scales the worst amongst the non brute-force methods. Unsurprisingly, the greedy method remains the fastest at large scale, although recall that the motivation of developing our method is for it to be distributed and that a greedy approach can not be distributed due to the global penalty term.

As for algorithm performance as it pertains to the cost of the obtained solution, we fix  $n = 50$  and additionally include DA variants of both NNN-C and NNN-D. We also omit the brute force method due to intractability. For the sake of comparison, we compute a performance metric  $Q$  and provide it for each method in Table 1. The metric  $Q$  is computed as follows: for each trial, sort the methods by solution cost. Assign a value of 6 for the best method, 5 for the second-best, and so on, down to the seventh-best (worst) receiving zero. Add up these scores for all 100 trials, and then normalize by a factor of 600 (the maximum possible score) to obtain  $Q$ . Note that  $Q$  does not account for runtime in any way.

It should be unsurprising that the tried-and-true centralized greedy and SDP methods perform the best. However, we note that they were beaten by our methods in a significant number of trials, which can be seen by noting that a  $Q$  score for two methods which perform best or second-best in all trials would sum to  $1100/600 = 1.83$ , while  $Q(\text{greedy}) + Q(\text{SDP}) = 1.75$ , or a cumulative pre-scaled score of 1050, indicating that our methods outperformed these methods in net 50 “placement spots” over the 100 trials. In general, we find that the DA version of the NNN algorithms obtains better solutions than the non-DA version, confirming the benefit of this approach. We also find that NNN-D generally outperforms NNN-C. It’s possible that an initially “selfish” trajectory in  $x$  is beneficial, which would neglect the global penalty until  $y$  adequately converges, although this is speculative. Lastly, we note that the HNN method never

Table 1

Comparison of performance metric  $Q$  for 100 randomized trials with  $n = 50$ .

Method	$Q$
NNN-c	0.2161
NNN-c-DA	0.2891
NNN-d	0.5443
NNN-d-DA	0.7005
HNN	0
Greedy	0.8411
SDP	0.9089

performs better than worst, which we attribute to the steepest-descent nature of gradient algorithms which do not use curvature information of the energy function. It might be possible that the stopping criterion forces HNN to terminate near saddle-points, although we do not suspect this since we observe the Hessian is positive-definite in the majority of termination instances.

As for parameter selection, we find that choosing  $m \ll 1$  is generally best, since  $m \geq 1$  would always produce a PT-inverse Hessian with eigenvalues contained in  $(0, 1]$ . This effectively scales down  $\dot{x}$  in the eigenspace associated with Hessian eigenvalue magnitudes greater than 1, but does not correspondingly scale up  $\dot{x}$  in the complementary eigenspace associated with small eigenvalues. Additionally, choosing  $T/\tau$  greater than 1 in the fixed case tended to be effective. This may be related to selecting  $a_i < -\gamma\|p\|^2 - 4T/\tau$  to guarantee anti-stability from  $(0.5)\mathbf{1}_n$ , and would explain why a high  $T_0/\tau_0$  that decreases in the DA learning variant performs so well. In general, for the DA learning variant, we recommend choosing  $T_0, \tau_0$  so that  $T_0/\tau_0 \gg 1$  and also  $\beta > 1$  sufficiently large so that  $T/\tau \ll 1$  by algorithm termination, which gives rise to a robust exploration/exploitation tradeoff. Finally, all  $\alpha \approx 1$  seem to behave roughly the same, with only  $\alpha \ll 1$  and  $\alpha \gg 1$  behaving poorly (the former leading to slow convergence in  $y$  and “selfish” behavior in  $x$ , and the latter being destabilizing in the discretization of  $\dot{y}$ ).

## 6.2 Learning Steps and 2-D Trajectories

Next, for the sake of understanding how the learning rate  $T/\tau$  affects the trajectories of the solutions, we have provided Figure 3 which plots the 2-D trajectories of NNN-C and NNN-D with  $T/\tau$  being gradually reduced over 15 learning steps. The contours of the energy function for the final step are also plotted. The problem data and choice for  $a$  is:

$$c = (2, 1)^\top, \quad p = (3, 1)^\top, \quad P_r = 2.8, \quad \gamma = 4, \\ a := -(10, 10)^\top.$$

Table 2

Problem data and parameter choices (where relevant) for performance comparison. Problem data  $p_i, c_i$  is generated randomly from given distributions for each of 100 trials.

Data or parameter	Value
$n$	50
$p_i$	$\mathcal{U}[1, 50]$
$c_i$	$p_i^e, e \sim \mathcal{U}[2, 3]$
$P_r$	1500
$\gamma$	1
$T_0$	1
$\tau_0$	0.1
$m$	0.1
$\alpha$	1
Learning steps	10
$\beta$	1.4
$n$	50

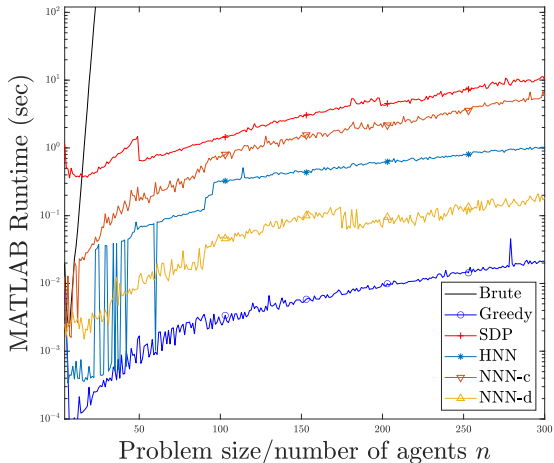


Fig. 2. Runtime of each method for increasing problem sizes.

Note that, in each case, the trajectory approaches the optimal solution  $x^* = (1, 0)^\top$ . However, it is worth noting that a steep saddle point occurs around  $x = (0.75, 0.6)^\top$ . Intuitively, this corresponds to a high risk of the trajectory veering away from the optimal solution had the DA not been implemented. With the opportunity to gradually learn the curvature of the energy function, as shown by stabilization to successive equilibria marked by  $\times$ , each algorithm is given the opportunity to richly explore the state space before stabilizing to the optimal solution  $(1, 0)^\top$ . Further studying the learning-rate  $T/\tau$  and a more complete analysis of Algorithm 1 and the parameter  $\beta$  are subjects of future work.

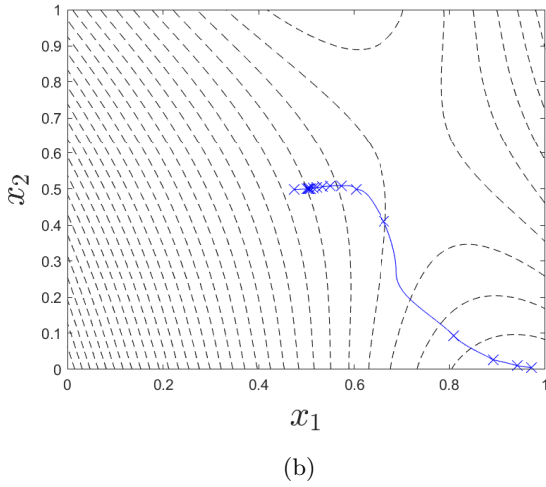
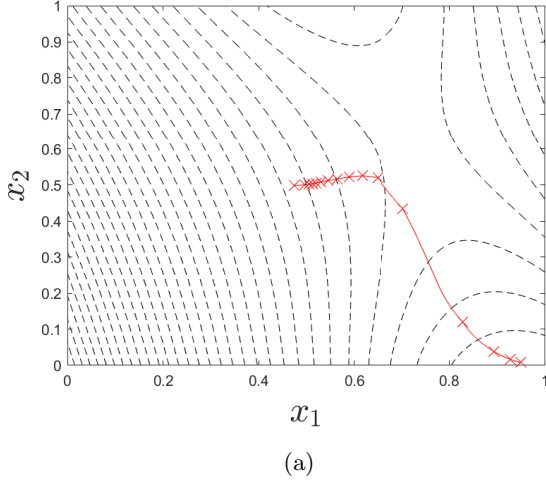


Fig. 3. Centralized NNN-C (a) and distributed NNN-D (b) trajectories in 2D with 15 learning steps. Stable equilibrium points between learning steps indicated by  $\times$ , contours of  $E$  and  $\tilde{E}$  in final step indicated by dashed lines.

## 7 Conclusion

This paper posed an optimal generator dispatch problem for settings in which the agents are generators with binary controls. We first showed that the centralized problem is amenable to solution via a Centralized NEWTON-LIKE NEURAL NETWORK approach and proved convergence to a local minimizer with probability one under light assumptions. Next, we developed an approach to make the dynamics computable in a distributed setting in which agents exchange messages with their two-hop neighbors in a communication graph. The methods scale and perform well compared to standard greedy and SDP-relaxation approaches, and the latter method enjoys the qualities of a distributed algorithm, unlike previous approaches. Future research directions include application of the methods to a broader class of

problems which may include additional cost terms or constraints and a deeper analysis of the Deterministic Annealing variant as it pertains to the online adjustment of the learning-rate  $T/\tau$ .

## Appendix

### *Proofs of Lemmas, Theorems, and Propositions*

**Proof of Lemma 2:** First consider only  $\mathcal{X} \cap (0, 1)^n$ . Note that  $(|H(x)|_m)^{-1} \succ 0$  (by construction) and  $\text{diag}((x_i - x_i^2)_i/T) \succ 0$  on  $x \in (0, 1)^n$ , so we focus on

$$Wx + \frac{T}{\tau} \log(1/x_i - 1)_i + v = \mathbf{0}_n. \quad (10)$$

Examining the above expression elementwise, it is non-constant, continuous, and its derivative changes sign only a finite number of times. Therefore, the total number of zeros on  $(0, 1)^n$  must be finite.

Now consider the  $i^{\text{th}}$  element of (10) for  $x_j \rightarrow 0$  or 1 for all  $j$  in an arbitrary permutation of  $\{1, \dots, n\} \setminus \{i\}$ . Since the number of these permutations is finite, and each permutation still gives rise to a finite number of solutions to (10) in the  $i^{\text{th}}$  component, it follows that  $\mathcal{X}$  is finite.  $\square$

**Proof of Lemma 3:** Consider again the terms of  $\dot{x}$  elementwise. There are two cases to consider for evaluating  $x_i$ :  $x_i = \varepsilon$  and  $x_i = 1 - \varepsilon$  for some  $0 < \varepsilon \ll 1$  sufficiently small such that the terms of  $(|H(x)|_m)^{-1}$  are still dominated by  $(1/x_i - x_i^2)$  and the  $Wx + v$  are still dominated by the log term. Then, consider the expression

$$\log(1/x_i - 1)(x_i - x_i^2)^2. \quad (11)$$

For  $x_i = \varepsilon \approx 0$ , (11) evaluates to a small positive value, and for  $x_i = 1 - \varepsilon \approx 1$ , (11) evaluates to a small negative value. We have argued that these are the dominating terms regardless of values of the remaining components of  $x$ , and so we conclude that  $x_i \in \{0, 1\}$  are componentwise anti-stable and that elements of  $x$  will never approach 0 or 1. Thus, the open hypercube is forward invariant.  $\square$

**Proof of Theorem 4:** Let  $\mathcal{X}$  be the set of all critical points of  $E$ . We first establish that  $E$  decreases along the trajectories of NNN-C and that  $x(t)$  converges asymptotically to  $\mathcal{X}$ . Differentiating  $E$  in time, we obtain:

$$\begin{aligned} \frac{dE}{dt} &= \dot{x}^\top \nabla_x E(x) = \dot{x}^\top (-Wx - v + g^{-1}(x)/\tau) \\ &= -\dot{x}^\top \text{diag}\left(\frac{T}{(x_i - x_i^2)_i}\right) |H(x)|_m \dot{x} < 0, \end{aligned} \quad (12)$$

for  $\dot{x} \neq 0$ ,  $x \in (0, 1)^n$ .

Recall that  $x(t) \in (0, 1)^n$  for all  $t \geq 0$  due to Lemma 3. From (4) and the discussion that followed on equilibria,  $\dot{x} = 0$  implies  $\nabla_x E(x) = 0$  due to  $(|H(x)|_m)^{-1} \succ 0$  and  $\text{diag}((x_i - x_i^2)_i / T) \succ 0$  on  $x \in (0, 1)^n$ . The domain of  $E$  is the compact set  $[0, 1]^n$  (per the definition of the integral terms), and  $E$  is continuous and bounded from below on this domain, so at least one critical point exists. Combining this basic fact with (12) shows that the NNN-C dynamics monotonically decrease  $E$  until reaching a critical point. More formally, applying the LaSalle Invariance Principle [21] tells us that the trajectories converge to the largest invariant set contained in the set  $dE/dt = 0$ . This set is  $\mathcal{X}$ , which is finite per Lemma 2. In this case, the LaSalle Invariance Principle additionally establishes that we converge to a single  $x^* \in \mathcal{X}$ .

The proof of the second statement of the theorem relies on an application of the Stable Manifold Theorem (see [14]) as well as Lemma 2. Let  $\hat{x} = \varphi_{T,\tau}(x)$  for a particular  $T, \tau$ . We aim to show that  $\mathbb{P}[\cup_{\hat{x}} \{\mathcal{W}_s(\hat{x}) \mid \hat{x} \text{ is a saddle or local maximum}\}] = 0$  under Assumptions 2-3. It is sufficient to show that, for each critical point  $x^*$  such that  $\varphi_{T,\tau}(x^*) = 0$ , and almost all  $T, \tau$ ,  $D\varphi_{T,\tau}(x^*)$  is full rank and its eigenvalues have non-zero real parts. The reason for this argument is the following: let  $x^*$  be a critical point with  $D\varphi_{T,\tau}(x^*)$  full rank and eigenvalues with non-zero real parts. If the eigenvalues do *not* all have positive real parts, then some have negative real parts, which indicates that  $x^*$  is a saddle or local maximum of  $E$ . These negative real-part eigenvalues induce an unstable manifold of dimension  $n_u \geq 1$ . As such, the globally stable set  $\mathcal{W}_s(x^*)$  is a manifold with dimension  $n - n_u < n$ , and  $\mathbb{P}[x(0) \in \mathcal{W}_s(x^*)] = 0$  per Assumption 2.

To argue this case, define  $h : (0, 1)^n \times \mathbb{R} \times \mathbb{R} \rightarrow \mathbb{R}$  as

$$h(x, T, \tau) = \det D\varphi_{T,\tau}(x).$$

We now leverage Assumption 3 and [25] to claim first that  $\mathbb{P}[h(x^*, T, \tau) = 0] = 0$  for each  $x^* \in \mathcal{X}$ , i.e.  $D\varphi_{T,\tau}(x^*)$  is full rank for each  $x^*$  with probability one w.r.t.  $\mathbb{P}$ . We first address the points  $x$  for which the function  $h$  is discontinuous. Define  $\hat{\mathcal{X}}$  as the set of  $x$  for which the truncation of the eigenvalues of  $H(x)$  becomes active, i.e. the discontinuous points of  $h$ . Although we do not write it as such, note that  $H$  is implicitly a function of  $T, \tau$  and that the eigenvalues of  $H$  can be expressed as nonconstant real-analytic functions of  $T, \tau$ . Considering this fact and an arbitrary  $x$ , the set of  $T, \tau$  which give  $x \in \hat{\mathcal{X}}$  has measure zero with respect to  $\mathbb{R}^2$  [25]. Thus, for particular  $T, \tau$ ,  $h$  is  $C^\infty$  almost everywhere. Applying once more the argument in [25] and Assumption 3 with the fact that  $h$  is a nonconstant real analytic function of  $T, \tau$  we have that

$$\bar{\mathbb{P}}[\mathcal{T}(\hat{x}) \triangleq \{(T, \tau) \mid h(\hat{x}, T, \tau) = 0\}] = 0, \quad \forall \hat{x} \notin \hat{\mathcal{X}}.$$

Now consider the set of critical points as an explicit function of  $T, \tau$  and write this set as  $\mathcal{X}(T, \tau)$ . Recalling Lemma 2, the set of  $\hat{x}$  that we are interested in reduces to a finite set of critical points  $x^* \in \mathcal{X}(T, \tau)$ . Thus, we can conclude that  $\bar{\mathbb{P}}(\cup_{x^* \in \mathcal{X}(T, \tau)} \mathcal{T}(x^*)) \leq \sum_{x^* \in \mathcal{X}(T, \tau)} \bar{\mathbb{P}}(\mathcal{T}(x^*)) = 0$ .

There is an additional case which must be considered, which is that  $h(x^*, T, \tau) \neq 0$ , but some eigenvalues of  $D\varphi_{T,\tau}(x^*)$  are purely imaginary and induce stable center manifolds, which could accommodate the case of a globally stable set which is an  $n$ -dimensional manifold (i.e. the “degenerate saddle” case). We consider the function  $h$  mostly out of convenience, but the argument can be extended to a function  $\mathbf{h} : (0, 1)^n \times \mathbb{R} \times \mathbb{R} \rightarrow \mathbb{C}^n$  which is a map to the roots of the characteristic equation of  $D\varphi_{T,\tau}(x)$ . We are concerned that each element of  $\mathbf{h}(x, T, \tau)$  should have a nonzero real part almost everywhere. To extend the previous case to this, consider the identification  $\mathbb{C} \equiv \mathbb{R}^2$  and compose  $\mathbf{h}$  with the nonconstant real analytic function  $\zeta(w, z) = w$ , for which the zero set is  $w \equiv 0$ , corresponding to the imaginary axis in our identification. From this, we obtain a nonconstant real-analytic as before whose zero set is the imaginary axis. Applying the argument in [25] in a similar way as above,  $\mathbf{h}(x, T, \tau)$  has nonzero real parts for almost all  $(T, \tau)$  for each  $x$ . Therefore, the probability of a particular saddle point or local maximum  $x^*$  having a nonempty stable center manifold is zero for arbitrary  $x(0)$  satisfying Assumption 2 and  $T, \tau$  satisfying Assumption 3.  $\square$

**Proof of Lemma 6:** The equivalence stems from the global term and the flexibility in the unconstrained  $y$  variable. Notice

$$\begin{aligned} \frac{\gamma}{2} \sigma^\top \sigma &= \frac{\gamma}{2} \sigma^\top (I_n - \mathbf{1}_n \mathbf{1}_n^\top / n) \sigma + \frac{\gamma}{2} \sigma^\top (\mathbf{1}_n \mathbf{1}_n^\top / n) \sigma \\ &= \frac{\gamma}{2} \sigma^\top (I_n - \mathbf{1}_n \mathbf{1}_n^\top / n) \sigma + \frac{\gamma}{2} (p^\top x - P_r)^2. \end{aligned}$$

We have recovered the original global term of  $\mathcal{P} 1$  in the bottom line, so now we deal with the remaining term. The matrix  $I_n - \mathbf{1}_n \mathbf{1}_n^\top / n \succeq 0$  has image  $I_n - \mathbf{1}_n \mathbf{1}_n^\top / n = \text{span}\{\mathbf{1}_n\}^\perp = \text{image } L$ , given that  $L$  is connected. Thus, because  $y$  is unconstrained and does not enter the cost anywhere else, we can compute the set of possible minimizers of  $\tilde{f}$  in closed form with respect to any  $x$  as

$$\begin{aligned} y^* &\in \{-L^\dagger((p_i x_i)_i - (P_r/n) \mathbf{1}_n) + \theta \mathbf{1}_n \mid \theta \in \mathbb{R}\} \\ &= \{-L^\dagger(p_i x_i)_i + \theta \mathbf{1}_n \mid \theta \in \mathbb{R}\}. \end{aligned}$$

Moreover, substituting a  $y^*$  gives  $\sigma \in \text{span}\{\mathbf{1}_n\}$ , and it follows that the problem  $\mathcal{P} 2$  reduces precisely to  $\mathcal{P} 1$ .  $\square$

**Proof of Lemma 7:** The proof is trivially seen by multiplying  $\dot{y}$  in (7) from the left by  $\mathbf{1}_n$  and applying the null space of  $L$ .  $\square$

**Proof of Lemma 8:** The first term is computed by setting  $\nabla_y \tilde{f}(x, y^*) = \mathbf{0}_n$  (resp.  $\nabla_y \tilde{E}(x, y^*) = \mathbf{0}_n$ ) and solving for  $y^*$ . There is a hyperplane of possible solutions due to the rank deficiency of  $L$ , but we are looking for the unique solution in  $\mathcal{Y}$ . The second term therefore follows from (8). The fact that this point is also the unique equilibrium in  $\mathcal{Y}$  follows from the fact that  $\dot{y} = -\alpha \nabla_y \tilde{E}(x, y^*)$ .  $\square$

**Proof of Lemma 9:** The proof follows closely to the proof of Lemma 2 with the variation that  $\tilde{v}$  in the expression for  $\dot{x}$  is now a function of  $y$ . Given the result of Lemma 8, we may directly substitute the unique  $y^*$  (9) for any  $x$ . Because  $y^*$  is simply a linear expression in  $x$ , the same argument as in Lemma 2 that  $\mathcal{X}$  is finite follows.  $\square$

**Proof of Theorem 10:** The first part of the proof to establish convergence to a critical point follows from a similar argument to the proof of Theorem 4. Differentiating  $\tilde{E}$  with respect to time gives:

$$\begin{aligned} \frac{d\tilde{E}}{dt} &= \begin{bmatrix} \dot{x} \\ \dot{y} \end{bmatrix}^\top \begin{bmatrix} \nabla_x \tilde{E}(x, y) \\ \nabla_y \tilde{E}(x, y) \end{bmatrix} \\ &= \begin{bmatrix} \dot{x} \\ \dot{y} \end{bmatrix}^\top \begin{bmatrix} -\tilde{W}x - \tilde{v} + g^{-1}(x)/\tau \\ -\alpha^{-1}\dot{y} \end{bmatrix} \\ &= -\dot{x}^\top \text{diag}(T/(x_i - x_i^2)_i) \tilde{H}(x)|_m \dot{x} - \alpha^{-1} \dot{y}^\top \dot{y} < 0, \\ &\quad \dot{x} \neq 0 \text{ or } \dot{y} \neq 0, \quad (x, y) \in (0, 1)^n \times \mathcal{Y}. \end{aligned} \quad (13)$$

Thus,  $\tilde{E}$  monotonically decreases along the trajectories of NNN-D. Given (13), we call again on the forward invariance property of the open hypercube for the distributed case via Lemma 11, which verifies that  $(x, y) \in (0, 1)^n \times \mathcal{Y}$  at all times.

Due to the deficiency induced by  $L$ ,  $\tilde{E}$  is not radially unbounded in  $y$  over all of  $\mathbb{R}^n$ , so we must be careful before applying the LaSalle Invariance Principle. Instead, define  $\tilde{E}$  only on  $[0, 1]^n \times \mathcal{Y}$  in consideration of Lemma 7. Radial unboundedness in  $\tilde{E}$  is then obtained given any  $y(0)$ , and it follows that the trajectories converge to largest invariant set contained in  $d\tilde{E}/dt = 0$  per the LaSalle Invariance Principle [21]. This is the finite set of critical points of  $\tilde{E}$  per Lemma 9, and so it additionally follows that we converge to a single critical point  $(x^*, y^*)$ .

Because  $\tilde{E}$  is convex in  $y$ , it follows that for any fixed  $x$  there exist only local minima of  $\tilde{E}$  with respect to  $y$ . In consideration of this, we need only apply the Stable Manifold Theorem [14] to  $x$ . The argument for this develops similarly to the proof of Theorem 4, and we conclude that the trajectories of NNN-D converge to a local

minimizer  $(x^*, y^*)$  of  $\tilde{E}$  with probability one.

The final part of the Theorem statement that  $\tilde{E}(x^*, y) \geq \tilde{E}(x^*, y^*)$ ,  $\forall y \in \mathbb{R}^n$  can also be seen from the convexity of  $\tilde{E}$  in  $y$  and applying the first-order condition of convexity:

$$\tilde{E}(x^*, y) \geq \tilde{E}(x^*, y^*) + (y - y^*)^\top \nabla_y \tilde{E}(x^*, y^*)$$

along with  $\nabla_y \tilde{E}(x^*, y^*) = \mathbf{0}_n$ .  $\square$

**Proof of Lemma 11:** The forward invariance of  $\mathcal{Y}$  is already established per its definition and Lemma 7, but we must establish that the trajectories  $y(t)$  remain bounded in order to apply the argument in Lemma 3 to the proof of Theorem 10. Compute the Hessian of  $\tilde{E}$  with respect to  $y$  as:

$$\nabla_{yy} \tilde{E} = \gamma L^2 \succeq 0.$$

Due to the connectedness of  $L$ , the eigenspace associated with the  $n - 1$  strictly positive eigenvalues of  $\gamma L^2$  is parallel to  $\mathcal{Y}$ . Therefore,  $\tilde{E}$  is strictly convex in  $y$  on this subspace, and it follows that  $\tilde{E}$  is bounded from below on  $\mathcal{Y}$ . Due to  $d\tilde{E}/dt \leq 0$  (13) and the continuity of  $\tilde{E}$  in  $y$ , it follows that  $y(t)$  is bounded for all  $t$ . Given this, the argument from Lemma 3 applies to the trajectories  $x(t)$ , and the set  $(0, 1)^n \times \mathcal{Y}$  is forward invariant under NNN-D (7).  $\square$

## References

- [1] CAISO business practice manual for market operation. <https://bpmcm.caiso.com/Pages/BPMDetails.aspx?BPM=Market%20Operations> 2018. Version 57.
- [2] S. Bauk and Z. Avramović. Hopfield network in solving travelling salesman problem in navigation. In *Seminar on Neural Network Applications in Electrical Engineering*, pages 207–210, 2002.
- [3] D. P. Bertsekas and J. Tsitsiklis. *Neuro-Dynamic Programming*. Athena Scientific, 1996.
- [4] S. Boyd and L. Vandenberghe. Semidefinite programming relaxations of non-convex problems in control and combinatorial optimization. In A. Paulraj, V. Roychowdhuri, and C. Schaper, editors, *Communications, Computation, Control and Signal Processing: A Tribute to Thomas Kailath*, chapter 15, pages 279–288. Kluwer Academic Publishers, 1997.
- [5] S. Boyd and L. Vandenberghe. *Convex Optimization*. Cambridge University Press, 2004.
- [6] F. Bullo, J. Cortés, and S. Martínez. *Distributed Control of Robotic Networks*. Applied Mathematics Series. Princeton University Press, 2009.
- [7] P. Chardaire and A. Sutter. A decomposition method for quadratic zero-one programming. *Management Science*, 41(4):704–712, 1995.
- [8] A. Cherukuri, E. Mallada, S. H. Low, and J. Cortés. The role of convexity in saddle-point dynamics: Lyapunov function and robustness. *IEEE Transactions on Automatic Control*, 63(8):2449–2464, 2018.

- [9] T. Cormen, C. Leiserson, R. Rivest, and C. Stein. *Introduction to Algorithms*. MIT Press, 3 edition, 2009.
- [10] Y. Dauphin, R. Pascanu, C. Gulcehre, K. Cho, S. Ganguli, and Y. Bengio. Identifying and attacking the saddle point problem in high-dimensional non-convex optimization. *International Conference on Neural Information Processing Systems*, pages 2933–2941, 2014.
- [11] P. Gill, W. Murray, and M. Wright. *Practical optimization*. Academic Press, 1981.
- [12] R. Goebel, R. G. Sanfelice, and A. Teel. Hybrid dynamical systems. *IEEE Control Systems Magazine*, 29(2):28–93, 2009.
- [13] M. Grant and S. Boyd. CVX: Matlab software for disciplined convex programming, version 2.1. <http://cvxr.com/cvx>, Mar. 2014.
- [14] J. Guckenheimer and P. Holmes. *Nonlinear Oscillations, Dynamical Systems, and Bifurcations of Vector Fields*. Springer, 1983.
- [15] G. Gutin, A. Yeo, and A. Zverovich. Traveling salesman should not be greedy: Domination analysis of greedy-type heuristics for the TSP. *Discrete Applied Mathematics*, 117(1-3):81–86, 2002.
- [16] X. He, X. Fang, and J. Yu. Distributed energy management strategy for reaching cost-driven optimal operation integrated with wind forecasting in multimicrogrids system. *IEEE Transactions on Systems, Man, & Cybernetics. Part A: Systems & Humans*, 49(8):1643–1651, 2019.
- [17] X. He, J. Yu, T. Huang, and C. Li. Distributed power management for dynamic economic dispatch in the multimicrogrids environment. *IEEE Transactions on Control Systems Technology*, 27(4):1651–1658, 2019.
- [18] J. Hopfield and D. Tank. Neural computation of decisions in optimization problems. *Biological Cybernetics*, 52(3):141–152, 1985.
- [19] B. Huang, L. Liu, H. Zhang, Y. Li, and Q. Sun. Distributed optimal economic dispatch for microgrids considering communication delays. *IEEE Transactions on Systems, Man, & Cybernetics. Part A: Systems & Humans*, 49(8):1634–1642, 2019.
- [20] B. Kamgar-Parsi and B. Kamgar-Parsi. Dynamical stability and parameter selection in neural optimization. In *International Joint Conference on Neural Networks*, page 566571, 1992.
- [21] H. Khalil. *Nonlinear Systems*. Prentice Hall, 2002.
- [22] D. Li, X. Sun, S. Gu, J. Gao, and C. Liu. Polynomially solvable cases of binary quadratic programs. In A. Chinchuluun, P. Pardalos, R. Enkhbat, and I. Tseveendorj, editors, *Optimization and Optimal Control*, pages 199–225. Springer, 2010.
- [23] Z. Q. Luo, W. K. Ma, A. So, Y. Ye, and S. Zhang. Semidefinite relaxation of quadratic optimization problems. *IEEE Signal Processing Magazine*, 27(3):2034, 2010.
- [24] J. Mandziuk. Solving the travelling salesman problem with a Hopfield-type neural network. *Demonstratio Mathematica*, 29(1):219–231, 1996.
- [25] B. Mityagin. The zero set of a real analytic function. *arXiv:1512.07276v1*, 2015.
- [26] G. L. Nemhauser, L. A. Wolsey, and M. L. Fisher. An analysis of approximations for maximizing submodular set functions-I. *Mathematical Programming*, 14(1):265–294, 1978.
- [27] V. Pan and Z. Chen. The complexity of the matrix eigenproblem. In *ACM Symposium on Theory of Computing*, pages 507–516, 1999.
- [28] P. Parrilo and S. Lall. Semidefinite programming relaxations and algebraic optimization in control. *European Journal of Control*, 9(2-3):307–321, 2003.
- [29] S. Poljak, F. Rendl, and H. Wolkowicz. A recipe for semidefinite relaxation for (0,1)-quadratic programming. *Journal of Global Optimization*, 7(1):51–73, 1995.
- [30] K. Rose. Deterministic annealing for clustering, compression, classification, regression, and related optimization problems. *Proceedings of IEEE*, 86(11):2210–2239, 1998.
- [31] S. Paternain, A. Mokhtari, and A. Ribeiro. A Newton-based method for nonconvex optimization with fast evasion of saddle points. *SIAM Journal on Optimization*, 29(1):343–368, 2019.
- [32] M. Shamaiah, S. Banerjee, and H. Vikalo. Greedy sensor selection: Leveraging submodularity. In *IEEE Int. Conf. on Decision and Control*, pages 2572–2577, 2010.
- [33] K. Smith. *Solving Combinatorial Optimization Problems Using Neural Networks*. PhD thesis, University of Melbourne, March 1996.
- [34] L. Vandenberghe and S. Boyd. Semidefinite programming. *SIAM Review*, 38(1):49–95, 1996.
- [35] P. Wang, C. Shen, A. Hengel, and P. Torr. Large-scale binary quadratic optimization using semidefinite relaxation and applications. *IEEE Transactions on Pattern Analysis and Machine Intelligence*, 39(3):470–485, 2017.
- [36] Z. Yang, A. Bose, H. Zhong, N. Zhang, Q. Xia, and C. Kang. Optimal reactive power dispatch with accurately modeled discrete control devices: A successive linear approximation approach. *IEEE Transactions on Power Systems*, 32(3):2435–2444, 2016.
- [37] P. Yi, Y. Hong, and L. Feng. Initialization-free distributed algorithms for optimal resource allocation with feasibility constraints and its application to economic dispatch of power systems. *Automatica*, 74:259–269, 2016.